Observation of photoassociation of ultracold sodium and cesium at the asymptote Na ($3S_{1/2}$) + Cs ($6P_{1/2}$)

Jizhou Wu, Wenliang Liu, Xiaofeng Wang, Jie Ma, Dan Li, Vladimir B. Sovkov, Liantuan Xiao, and Suotang Jia

Citation: The Journal of Chemical Physics **148**, 174304 (2018); doi: 10.1063/1.5023330
View online: https://doi.org/10.1063/1.5023330
View Table of Contents: http://aip.scitation.org/toc/jcp/148/17
Published by the American Institute of Physics

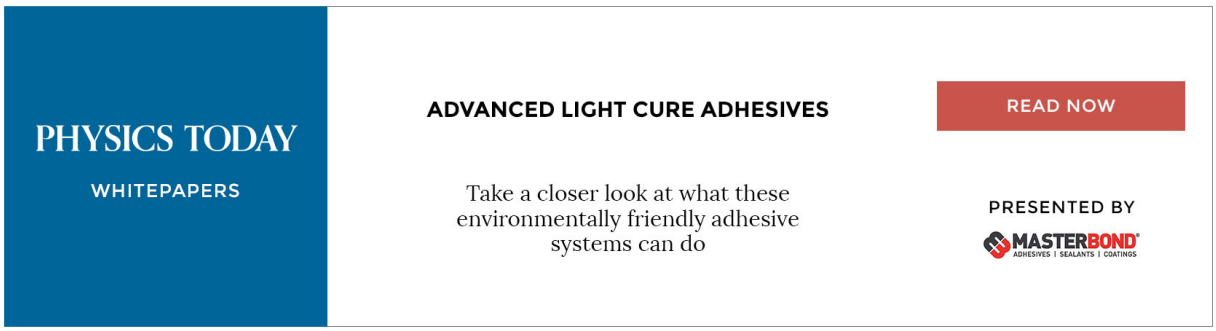

Observation of photoassociation of ultracold sodium and cesium at the asymptote Na ($3S_{1/2}$) + Cs ($6P_{1/2}$)

Jizhou Wu,[1,2] Wenliang Liu,[1] Xiaofeng Wang,[1] Jie Ma,[1,2,a)] Dan Li,[3] Vladimir B. Sovkov,[1,4,b)] Liantuan Xiao,[1,2] and Suotang Jia[1,2]

[1]*State Key Laboratory of Quantum Optics and Quantum Optics Devices, Institute of Laser Spectroscopy, College of Physics and Electronics Engineering, Shanxi University, Taiyuan 030006, China*
[2]*Collaborative Innovation Center of Extreme Optics, Shanxi University, Taiyuan, Shanxi 030006, People's Republic of China*
[3]*Center for Photonics and Electronics, Department of Precision Instruments, Tsinghua University, Beijing 100084, China*
[4]*St. Petersburg State University, 7/9 Universitetskaya Nab., St. Petersburg 199034, Russia*

(Received 23 January 2018; accepted 16 April 2018; published online 2 May 2018)

We report on the production of ultracold heteronuclear NaCs* molecules in a dual-species magneto-optical trap through photoassociation. The electronically excited molecules are formed below the Na ($3S_{1/2}$) + Cs ($6P_{1/2}$) dissociation limit. 12 resonance lines are detected using trap-loss spectroscopy based on a highly sensitive modulation technique. The highest observed rovibrational level exhibits clear hyperfine structure, which is detected for the first time. This structure is simulated within a simplified model consisting of 4 coupled levels belonging to the initially unperturbed Hund's case "*a*" electronic states, which have been explored in our previous work that dealt with the Na ($3S_{1/2}$) + Cs ($6P_{3/2}$) asymptote [W. Liu *et al.*, Phys. Rev. A **94**, 032518 (2016)]. *Published by AIP Publishing.*
https://doi.org/10.1063/1.5023330

I. INTRODUCTION

Recently, immense interest has been focused on the production and investigation of ultracold heteronuclear polar molecules due to their intrinsic permanent electric dipole moment in the rovibrational ground states and their long-range anisotropic dipole-dipole interactions, both of which are inaccessible in ultracold atomic systems.[1] These novel features have made the polar molecules ideal candidates for precision measurements,[2] quantum computation,[3] quantum chemical reactions,[4] and quantum simulation of condensed matter systems.[5,6] In recent decades, significant successes have been witnessed in the creation of ultracold fermionic $^{40}K^{87}Rb$[7] and $^{23}Na^{40}K$[8] molecules and bosonic $^{87}Rb^{133}Cs$[9,10] and $^{23}Na^{87}Rb$[11] molecules, all of which were achieved by coherently transferring the weakly bound Feshbach molecules via a Stimulated Raman Adiabatic Passage (STIRAP) to their absolute rovibrational ground states.

Most of the studies on the ground electronic states of heteronuclear polar molecules have been achieved, e.g., by spontaneous decay in the case of RbCs[12] and LiCs[13] or by using an auxiliary laser which couples the excited molecular state to a ground state as for KRb,[14] but efforts are still required to obtain precise knowledge of the excited electronic molecular structures.[15] Photoassociation (PA) has served as a simple and rapid approach to produce ultracold molecules far below 1 mK.[16] Meanwhile, high resolution PA spectroscopy (PAS) has enabled the obtainment of rich information about molecular structures and the precise measurement of the fundamental physical constants including their hypothetical time variation[17–20] and the *s*-wave scattering lengths.[21–23]

PA of ultracold polar molecules has been realized in diatomic species with different combinations of alkali metals (i.e., LiNa, LiCs, LiRb, KRb, NaK, and RbCs)[13,24–29] or alkaline-earth metals (i.e., RbYb and LiYb),[22,30,31] whose excited molecular states at large inter-nuclear separations present a van der Waals potential proportional to $1/R^6$ (where R is the nuclear distance). The NaCs molecule possesses the second largest permanent electric dipole moment (4.6 D[32]) among all the heteronuclear alkali diatomic molecules, and its ground state is expected to be stable against two-body inelastic collisions.[33,34] It should be noted that the strong spin-orbit mixing in the excited $A^1\Sigma^+ - b^3\Pi$ state complex of NaCs can lead to large vibrational wave function perturbations,[35] which facilitate radiative stabilization directly into the vibrational ground states. Finally, as NaCs molecules have only one stable bosonic isotopomer, these systems are prospects for the Bose-Einstein Condensation (BEC) of polar molecules. These distinctive merits made the NaCs molecules intriguing for various ultracold molecule applications.[36]

Due to these characteristics, a number of spectroscopic investigations on NaCs have been performed in hot molecular samples during the recent years, and various states, i.e., the $3^1\Pi$, $A^1\Sigma$, $b^3\Pi$, $X^1\Sigma^+$, $a^3\Sigma^+$, $5^3\Pi_0$, and $12(0^+)$ states of NaCs, have been analyzed.[35,37–41] Nevertheless, at a lower temperature far below 1 mK, the ultracold polar NaCs molecules demonstrate their advantages with enhanced accuracy and resolution. By using the PA approach, the ultracold NaCs molecules were created by Bigelow and co-workers for the first time.[42] Photoassociation spectra for several electronic states of NaCs molecules, i.e., the $1^1\Sigma^+$,[42] the $c^3\Sigma^+$,[43] the $B^1\Pi$,

[a)]Electronic mail: mj@sxu.edu.cn
[b)]Electronic mail: vladimir_sovkov@mail.ru

and the $X^1\Sigma^+$[44] states, had been obtained using the ionization detection technique.[45,46] Ground-state NaCs molecules have been reached by the decay following the PA process[46] or by optical pumping approaches.[47] Although featured by its zero-background signal and high sensitivity, the ionization method can only detect partial molecular states and does not provide useful molecular information such as PA transition intensities due to the interference from the ionization laser.[48] As an alternative approach to obtain the PAS, the trap-loss detection technique,[49] which directly monitors the fluorescence from the trapped ultracold atoms, is feasible for characterizing the majority of the electronic states in NaCs. High-resolution trap-loss spectroscopy (TLS) provides precise binding energy data for molecular rovibrational levels. In addition, it conveys rich information about their relative transition strengths,[50] which is of key importance to understand ultracold collisions, to verify *ab initio* theoretical predictions and to perform quantum simulations based on the creation of ultracold NaCs ground state molecules.

However, as the Franck-Condon factors (FCFs) of PA transitions are extremely small for heteronuclear molecules and the sensitivity of trap-loss detection is not sufficiently high, there were previously few reports on TLS for NaCs molecules.[51,52] Detailed studies on NaCs molecular TLS, especially for the mixed $A^1\Sigma^+ - b^3\Pi$ singlet-triplet states and for the molecular hyperfine structures, are required for many potential applications of ultracold polar molecules.[52,53]

In this paper, we demonstrate the high-resolution trap-loss spectroscopy of ultracold polar NaCs molecules below the Na $(3S_{1/2})$ + Cs $(6P_{1/2})$ asymptote (corresponding to the cesium atomic D_1 line at 894 nm), which are induced by the PA of a dual-species Na–Cs magneto-optical trap (MOT) using a modulation spectroscopy technique.[52] 12 rovibrational levels were observed, whose electronic components have a blended nature with prevailing $A^1\Sigma^+$ and $b^3\Pi$ characters. The hyperfine structure of the highest observed ro-vibrational level is registered and analyzed. Although the computational model is simple, it reproduces the overall characteristics of the hyperfine structure in the experimental spectrum.

This paper is organized as follows. In Sec. II, we briefly overview the experimental schemes and the setup. In Sec. III, we demonstrate the experimental results for the PAS of the 12 rovibrational levels of NaCs molecules. The theoretical model simulations for the observed hyperfine structures are presented in Sec. IV. Finally, the conclusions are given in Sec. V.

II. EXPERIMENT

As Fig. 1 depicts schematically, the experiment was carried out in a dual-species Na-Cs apparatus; most of these details were described in our studies on the $c^3\Sigma^+$ excited state of NaCs below the dissociation limit $3S_{1/2} + 6P_{3/2}$.[52] Here, we present some key characteristics of the setup.

A mixture of ultracold sodium and cesium atomic species was loaded and confined in a rectangular transparent quartz vacuum chamber with a background pressure of 1×10^{-8} Pa. Dark-spot magneto-optical traps (dark-SPOTs)[42] were overlapped at the center of the chamber for both species to provide the cold samples with a high atomic density and a low collision rate. The ^{23}Na (^{133}Cs) dark-SPOT typically contains an atomic number of $N_{Na} \sim 9 \times 10^6$ atoms ($N_{Cs} \sim 6 \times 10^7$) with a density of $n_{Na} \sim 2.0 \times 10^9$ cm^{-3} ($n_{Cs} \sim 1.5 \times 10^9$ cm^{-3}).

In the dark-SPOTs, the Na (Cs) atoms were mainly populated at the lower hyperfine level $F = 1$ ($F = 3$) of the $3S_{1/2}$ ($6S_{1/2}$) state. However, a contribution from the Na $F = 2$ state was also indicated in the experiment (see below), when the temperature was ~200 μK (~120 μK), which was measured using the time-of-flight method. Photoassociation was induced by a cw tunable Ti: sapphire laser system (MBR110) with a typical linewidth of less than 100 kHz and an output power up to ~3.5 W. A diode laser with an output at 532 nm (Verdi-18, a maximum power of ~18 W) served as the pumping laser. The PA laser beam was collimated to a $1/e^2$ diameter of 0.78 mm with a maximum available average intensity of ~750 W/cm^2. The absolute frequency of the PA laser was monitored and measured using a commercial wavelength meter (High Finesse-Angstrom, WS/U) with an accuracy of 30 MHz. The

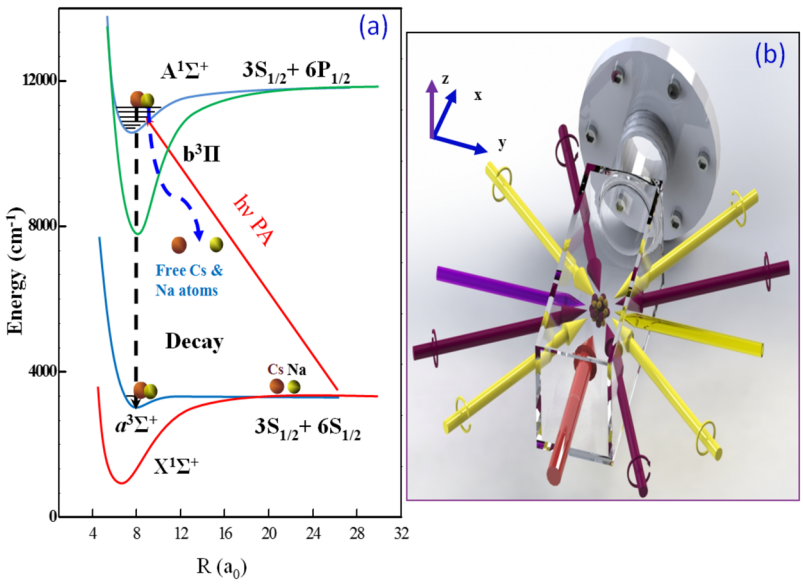

FIG. 1. (a) Schematic diagram of the PA process. Potential energy curves for NaCs below the $3S_{1/2}$ + $6P_{1/2}$ asymptote and the transition branches in the PA process are demonstrated. (b) The experimental geometry and the laser configuration used in the dual species MOT. Colorful lines in the x and y planes are the $\sigma^{+/-}$ circularly polarized cooling laser beams for the Na (yellow) and Cs (purple) MOTs, respectively. Repumping laser beams for the Na and Cs MOTs counter-propagated along the y axis, and their centers were both blocked with a hole of 5 mm. The depumping laser beams, as well as the vertical cooling laser beams, are not shown. PA laser beam (brown) transmits through the square window of the quartz cell and interacts with the Na–Cs MOTs.

wavelength meter was calibrated against the Cs atomic hyperfine resonant transition, $6S_{1/2}(F = 4) \rightarrow 6P_{1/2}(F' = 4)$, which corresponds to a wave number of 11 178.151 cm^{-1}.

As the simplest technique for detecting a PA transition, trap-loss detection is accomplished by monitoring the number of the trapped atoms remaining in the MOT. The formation of ultracold polar NaCs molecules leads to losses for both trapped Na and Cs atoms. In this way, the photoassociation process influences the balance of the numbers of atoms between the loading and loss processes by inducing an additional loss mechanism. By recording the variation of the DC voltage while fluorescence was emitted from the atoms along with the corresponding PA laser frequency, the number of trapped atoms in the MOT is measured. Thus, a typical PA spectrum is acquired.[54] Fluorescence from the Cs and Na dark-SPOT is collected separately: for the Cs atoms, an avalanche photodiode (APD) along with a convex lens was utilized, while a photo-multiplier (PMT) was used for the Na atoms to increase the detection sensitivity. Bandpass filters (852 nm for Cs and 589 nm for Na) were placed over the APD and PMT, respectively; the purpose was to shield stray light from the environment. Lock-in technology was used to improve the detection sensitivity of trap-loss spectroscopy by modulating the fluorescence of the ultracold atoms[50,55,56] with modulation frequencies of 3.2 kHz (3.4 kHz) for Na (Cs) atoms. Two lock-in amplifiers (Stanford Research SR830) were utilized to demodulate the fluorescence, which was recorded along with the PA laser frequency by a computer.

PA resonance leads to the formation of ultracold polar NaCs molecules in an electronic excited state and to the losses for both the trapped Na and Cs atoms. By monitoring the loss of Na's atomic fluorescence signal, the PAS for ultracold polar NaCs molecules are precisely obtained. The maximum loss ratio of the signal is about 0.55.

III. EXPERIMENTAL RESULTS

The trap-loss spectra are shown in Figs. 2 and 3. The abscissas give the energies relative to the limit of

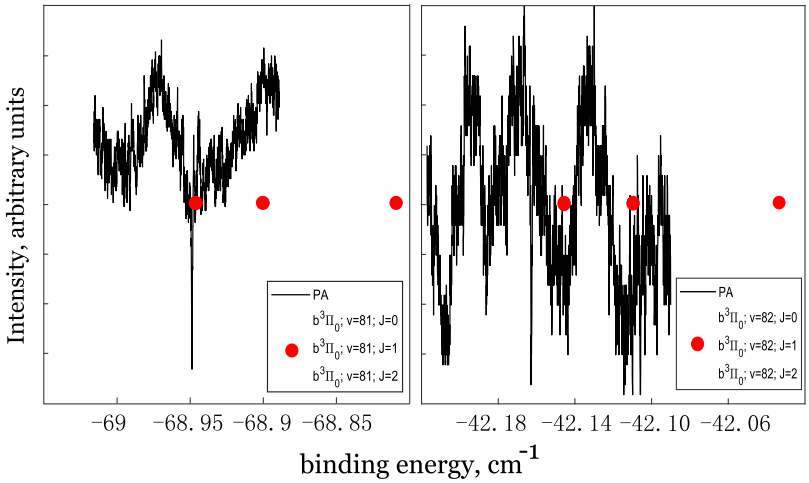

FIG. 2. The experimental PA trap-loss spectra (solid lines) of the NaCs $b^3\Pi$ (v = 81 and 82) state. As a comparison, the ro-vibrational term values assigned by Zabawa[57] are shown as the dots; the inset legends show the assignments from Ref. 57.

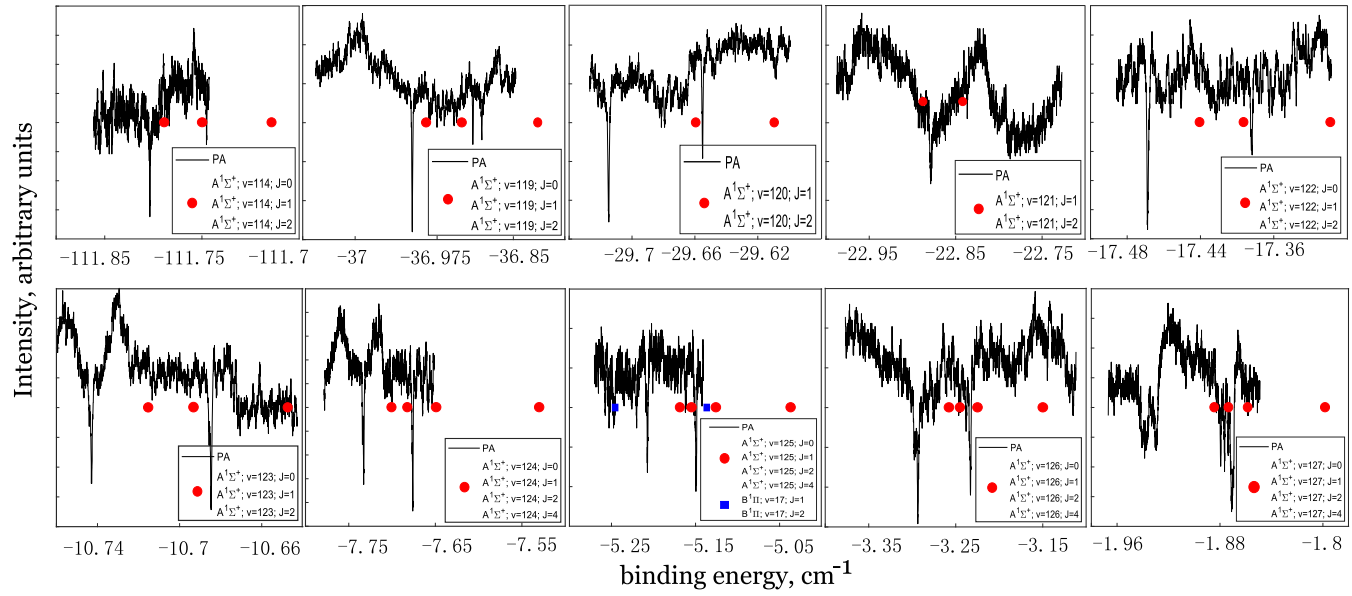

FIG. 3. The PA trap-loss spectra (solid lines) of the NaCs $A^1\Sigma^+$ (v = 114, and 119-127) state. For comparison, the dots are the ro-vibrational term values assigned by Zabawa,[57] while the squares are the neighboring $B^1\Pi$ (v = 17) state. The inset legends show the assignments from Ref. 57.

Na ($3S_{1/2}$) + Cs ($6P_{1/2}$). Besides our experimental data, we also show in Figs. 2 and 3 the binding energies reported in Ref. 57 (circles) with their electronic and ro-vibrational assignments (see legends), which are the closest values to our observed resonances. Almost all our spectra exhibited pairs of peaks (collections of peaks) separated by ∼1.8 GHz. This value is equal to the gap between the Na $F = 1$ and $F = 2$ states. Hence, we interpret the left peaks as transitions from the scattering state Na ($F = 2$) + Cs ($F = 3$), which obviously has not totally decayed in our sodium dark-SPOT. However, we have accepted the electronic and ro-vibrational assignments proposed in Ref. 43 for our PA resonances. In this context, we must emphasize that attributing near-dissociation levels to a definite Hund's case "*a*" electronic state is simply done out of convention: in fact, they are blends of components from different electronic characters caused by the fine and hyperfine coupling.

It is known that the strong PA laser field in the MOT is able to cause frequency shifts of the observed transitions,[58] but their characteristic values are noticeably less than the natural linewidths, and their registration requires special experimental techniques, which were not employed in the present work.

The highest observed level (the tentative assignment is $A^1\Sigma^+$, $v = 127$, $J = 1$) exhibits clear hyperfine structure. To the best of our knowledge, this structure was registered for the first time by us. The results of the simulation of this hyperfine structure are described in Sec. IV.

IV. MODEL SIMULATION

We have used the same simplified model, which was applied to the PA spectra for NaCs near the Na ($3S_{1/2}$) + Cs ($6P_{3/2}$) asymptote in our previous work.[52] The main idea was to consider 4 initially unperturbed levels belonging to the Hund's case "*a*" electronic states with symmetries of $^1\Sigma$, $^3\Sigma$, $^1\Pi$, and $^3\Pi$ and to mix them with various fine and hyperfine mechanisms. The relative positions of these levels are fitted to get the best reproduction of the experimental spectrum; the coupling parameters are also slightly adjusted, but they maintain magnitudes close to the values at the atomic limit. In the present work, we also adjusted the rotational constants of the levels, while trying to keep them close to the estimates based on the results from Ref. 57. The intensities are computed for transitions from the *s*-wave states of the lowest atomic limit with the help of the appropriate equations presented in Ref. 52. It is obvious that such a model is more qualitative than quantitative; however, this model allows one to reveal the physical mechanisms underlying the observations. A more elaborate quantitative model must involve the interactions between different vibrational states, which could be achieved via solving a multichannel Schrödinger equation; this would require far more intense computations. All the details and the necessary equations are contained in Ref. 52.

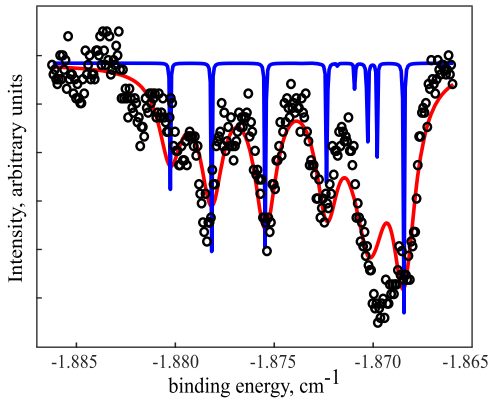

FIG. 4. The experimental trap-loss spectrum (circles) for the transition from the scattering state Na ($3S_{1/2}$, $F = 1$) + Cs ($6S_{1/2}$, $F = 3$) to the molecular ro-vibrational level NaCs ($A^1\Sigma^+$, $v = 127$, $J = 1$) with hyperfine structure and its simulation with low (red curve) and high (blue curve) resolution, respectively.

The strong spin-orbit (fine) coupling splits the modeled levels into two largely separated groups that belong to the limits of Na ($3S_{1/2}$) + Cs ($6P_{1/2}$) and Na ($3S_{1/2}$) + Cs ($6P_{3/2}$). In Ref. 52, we tracked the levels of the higher [Na ($3S_{1/2}$) + Cs ($6P_{3/2}$)] group, while in the present work, we tracked the levels of the lower [Na ($3S_{1/2}$) + Cs ($6P_{1/2}$)] group. Turning on the hyperfine interaction reveals the hyperfine structure of the levels. Our final simulations of the peaks belonging to transitions to the Na ($F = 1$) + Cs ($F = 3$) state (the right part of the bottom panel of Fig. 3) are shown in Fig. 4. The comparison between the experimental spectrum and the simulation is not ideal, but it is quite satisfactory for such a restricted mathematical model. Notice that most of the high-resolution lines in Fig. 4 are separated by intervals less than their natural linewidths, i.e., 15.02 MHz, which equals the sum of the natural linewidths of the Cs atom (5.23 MHz) and the Na atom (9.79 MHz) and is close to the observed experimental linewidths; thus, they are indistinguishable physically.

The computed individual hyperfine components on the NaCs ($A^1\Sigma^+$, $v = 127$, $J = 1$) level are listed in Table I, where they are labeled by the only one strict quantum number F. Notice that two of the high-resolution lines ($E = 1.8725$ cm^{-1} and $E = 1.8686$ cm^{-1}) in Fig. 4 are in fact unresolved double lines.

All the model peaks in Fig. 4 represent hyperfine molecular sublevels of the blended electronic nature, mostly $^1\Sigma$ and $^3\Pi$ with small intermixes of $^3\Sigma$ and $^1\Pi$. The fractions of the $^3\Pi$ character are larger than the fractions of the $^1\Sigma$ character despite the assignment of the level as the one belonging to the $A^1\Sigma^+$ state; we assume that this could be an artifact of our modeling, although a strong coupling of the $A^1\Sigma^+$ and $b^3\Pi$ states is

TABLE I. Computed individual hyperfine components on the ($A^1\Sigma^+$, $v = 127$, $J = 1$) level: binding energy E cm^{-1} versus the strict quantum number F.

E	1.8804	1.8783	1.8756	1.8726	1.8725	1.8719	1.8711	1.8704	1.8700	1.868 62	1.868 61
F	2	3	4	1	5	2	3	3	4	4	5

indeed expected (see the Introduction). Rather surprising for us was the fact that all these sublevels possessed more than 0.9 of the character for the rotational state $J = 1$, which confirmed the rotational assignment that was initially based on comparison of our results with those from Ref. 57. The dominant quantum number Ω is zero (otherwise noticeable contributions from the $A^1\Sigma^+$ state would be impossible). The strict quantum number F for the hyperfine sublevels spanning values from $F = 1$ to $F = 5$ is listed in Table I.

V. CONCLUSIONS

We have observed the trap-loss spectra for 12 rovibrational levels in ultracold NaCs heteronuclear molecules below the $3S_{1/2} + 6P_{1/2}$ asymptote. The hyperfine structure of the highest observed level $A^1\Sigma^+$ ($\upsilon = 127$, $J = 1$) is recorded for the first time. This hyperfine structure is simulated within a simplified model containing four coupled levels belonging to different initially unperturbed Hund's case "a" electronic states. The simulation illustrates that the level possesses mixed electronic nature with dominant character from the $A^1\Sigma^+$ and $b^3\Pi$ states.

ACKNOWLEDGMENTS

This work was supported by the National Key Research and Development Program of China (Grant No. 2017YFA0304203), the Chang Jiang Scholars and Innovative Research Team in the University of the Ministry of Education of China (Grant No. IRT13076), the National Natural Science Foundation of China (Grants Nos. 61722507, 61675121, 61705123, 11434007, and 11604177), the fund for Shanxi "1331 Project" Key Subjects Construction, the foundation for Outstanding Young Scholars of Shanxi Province, China (Grant No. 201601D021001), the outstanding young academic leader of Shanxi Province, the Applied Basic Research Project of Shanxi Province, China (Grant No. 201701D221002), the Fund Program for the Scientific Activities of Selected Returned Overseas Professionals in Shanxi Province, and collaborative grant by the Russian Foundation for Basic Research and NNSF of China (No. 18-53-53030 in the RFBR classification).

[1] L. D. Carr, D. DeMille, R. V. Krems, and J. Ye, New J. Phys. **11**, 055049 (2009).
[2] J. Baron, W. C. Campbell, D. DeMille, J. M. Doyle, G. Gabrielse, Y. V. Gurevich, P. W. Hess, N. R. Hutzler, E. Kirilov, I. Kozyryev, B. R. OLeary, C. D. Panda, M. F. Parsons, E. S. Petrik, B. Spaun, A. C. Vutha, and A. D. West, Science **343**, 269 (2014).
[3] D. DeMille, Phys. Rev. Lett. **88**, 067901 (2002).
[4] J. L. Bohn, A. M. Rey, and J. Ye, Science **357**, 1002 (2017).
[5] I. Bloch, J. Dalibard, and S. Nascimbéne, Nat. Phys. **8**, 267 (2012).
[6] I. Georgescu, S. Ashhab, and F. Nori, Rev. Mod. Phys. **86**, 153 (2014).
[7] K. K. Ni, S. Ospelkaus, M. H. G. de Miranda, A. Peer, B. Neyenhuis, J. J. Zirbel, S. Kotochigova, P. S. Julienne, D. S. Jin, and J. Ye, Science **322**, 231 (2008).
[8] J. W. Park, S. A. Will, and M. W. Zwierlein, Phys. Rev. Lett. **114**, 205302 (2015).
[9] P. K. Molony, P. D. Gregory, Z. Ji, B. Lu, M. P. Köppinger, C. R. Le Sueur, C. L. Blackley, J. M. Hutson, and S. L. Cornish, Phys. Rev. Lett. **113**, 255301 (2014).
[10] T. Takekoshi, L. Reichsöllner, A. Schindewolf, J. M. Hutson, C. R. Le Sueur, O. Dulieu, F. Ferlaino, R. Grimm, and H.-C. Nägerl, Phys. Rev. Lett. **113**, 205301 (2014).
[11] M. Guo, B. Zhu, B. Lu, X. Ye, F. Wang, R. Vexiau, N. Bouloufa-Maafa, G. Quéméner, O. Dulieu, and D. Wang, Phys. Rev. Lett. **116**, 205303 (2016).
[12] J. M. Sage, S. Sainis, T. Bergeman, and D. DeMille, Phys. Rev. Lett. **94**, 203001 (2005).
[13] J. Deiglmayr, A. Grochola, M. Repp, K. Mörtlbauer, C. Glück, J. Lange, O. Dulieu, R. Wester, and M. Weidemüller, Phys. Rev. Lett. **101**, 133004 (2008).
[14] K. Aikawa, D. Akamatsu, M. Hayashi, K. Oasa, J. Kobayashi, P. Naidon, T. Kishimoto, M. Ueda, and S. Inouye, Phys. Rev. Lett. **105**, 203001 (2010).
[15] J. Ulmanis, J. Deiglmayr, M. Repp, R. Wester, and M. Weidemüller, Chem. Rev. **112**, 4890 (2012).
[16] K. M. Jones, E. Tiesinga, P. D. Lett, and P. S. Julienne, Rev. Mod. Phys. **78**, 483 (2006).
[17] D. DeMille, S. Sainis, J. Sage, T. Bergeman, S. Kotochigova, and E. Tiesinga, Phys. Rev. Lett. **100**, 043202 (2008).
[18] T. Zelevinsky, S. Kotochigova, and J. Ye, Phys. Rev. Lett. **100**, 043201 (2008).
[19] S. Sainis, J. Sage, E. Tiesinga, S. Kotochigova, T. Bergeman, and D. DeMille, Phys. Rev. A **86**, 022513 (2012).
[20] K. Beloy, A. Borschevsky, V. V. Flambaum, and P. Schwerdtfeger, Phys. Rev. A **84**, 042117 (2011).
[21] J. Kim, S. Moal, M. Portier, J. Dugué, M. Leduc, and C. Cohen-Tannoudji, Europhys. Lett. **72**, 548 (2005).
[22] M. Borkowski, P. S. Żuchowski, R. Ciuryło, P. S. Julienne, D. Kędziera, Ł. Mentel, P. Tecmer, F. Münchow, C. Bruni, and A. Görlitz, Phys. Rev. A **88**, 052708 (2013).
[23] E. R. I. Abraham, W. I. McAlexander, C. A. Sackett, and R. G. Hulet, Phys. Rev. Lett. **74**, 1315 (1995).
[24] T. M. Rvachov, H. Son, A. T. Sommer, S. Ebadi, J. J. Park, M. W. Zwierlein, W. Ketterle, and A. O. Jamison, Phys. Rev. Lett. **119**, 143001 (2017).
[25] S. Dutta, J. Lorenz, A. Altaf, D. S. Elliott, and Y. P. Chen, Phys. Rev. A **89**, 020702(R) (2014).
[26] S. Dutta, J. Pérez-Ríos, D. S. Elliott, and Y. P. Chen, Phys. Rev. A **95**, 013405 (2017).
[27] D. Wang, J. Qi, M. F. Stone, O. Nikolayeva, H. Wang, B. Hattaway, S. D. Gensemer, P. L. Gould, E. E. Eyler, and W. C. Stwalley, Phys. Rev. Lett. **93**, 243005 (2004).
[28] J. W. Park, S. A. Will, and M. W. Zwierlein, New J. Phys. **17**, 075016 (2015).
[29] A. J. Kerman, J. M. Sage, S. Sainis, T. Bergeman, and D. DeMille, Phys. Rev. Lett. **92**, 033004 (2004).
[30] N. Nemitz, F. Baumer, F. Münchow, S. Tassy, and A. Görlitz, Phys. Rev. A **79**, 061403 (2009).
[31] R. Roy, R. Shrestha, A. Green, S. Gupta, M. Li, S. Kotochigova, A. Petrov, and C. H. Yuen, Phys. Rev. A **94**, 033413 (2016).
[32] M. Aymar and O. Dulieua, J. Chem. Phys. **122**, 204302 (2005).
[33] P. S. Julienne, T. M. Hannaa, and Z. Idziaszekb, Phys. Chem. Chem. Phys. **13**, 19114 (2011).
[34] M. Mayle, G. G. Quéméner, B. P. Ruzic, and J. L. Bohn, Phys. Rev. A **87**, 012709 (2013).
[35] J. Zaharova, M. Tamanis, R. Ferber, A. N. Drozdova, E. A. Pazyuk, and A. V. Stolyarov, Phys. Rev. A **79**, 012508 (2009).
[36] J. Kleinert, C. Haimberger, P. J. Zabawa, and N. P. Bigelow, Phys. Rev. Lett. **99**, 143002 (2007).
[37] U. Diemer, H. Weickenmeier, M. Wahl, and W. Demtröder, Chem. Phys. Lett. **104**, 489 (1984).
[38] O. Docenko, M. Tamanis, J. Zaharova, R. Ferber, A. Pashov, H. Knöckel, and E. Tiemann, J. Chem. Phys. **124**, 174310 (2006).
[39] O. Docenko, M. Tamanis, J. Zaharova, R. Ferber, A. Pashov, H. Knöckel, and E. Tiemann, J. Phys. B: At., Mol. Opt. Phys. **39**, S929–S943 (2006).
[40] S. Ashman, B. McGeehan, C. M. Wolfe, C. Faust, K. Richter, J. Jones, A. P. Hickman, and J. Huennekens, J. Chem. Phys. **136**, 114313 (2012).
[41] C. Faust, J. Jones, J. Huennekens, and R. W. Field, J. Chem. Phys. **146**, 104302 (2017).
[42] J. P. Shaffer, W. Chalupczak, and N. P. Bigelow, Phys. Rev. A **60**, 3365 (1999).
[43] A. Grochola, P. Kowalczyk, J. Szczepkowski, W. Jastrzebski, A. Wakim, P. Zabawa, and N. P. Bigelow, Phys. Rev. A **84**, 012507 (2011).
[44] P. Zabawa, A. Wakim, M. Haruza, and N. P. Bigelow, Phys. Rev. A **84**, 061401 (2011).
[45] A. Wakim, P. Zabawa, and N. P. Bigelow, Phys. Chem. Chem. Phys. **13**, 18887 (2011).

[46]C. Haimberger, J. Kleinert, M. Bhattacharya, and N. P. Bigelow, Phys. Rev. A **70**, 021402 (2004).
[47]A. Wakim, P. Zabawa, M. Haruza, and N. P. Bigelow, Opt. Express **20**, 16083 (2012).
[48]E. Tiesinga, K. M. Jones, P. D. Lett, U. Volz, C. J. Williams, and P. S. Julienne, Phys. Rev. A **71**, 052703 (2005).
[49]D. Comparat, C. Drag, A. Fioretti, O. Dulieu, and P. Pillet, J. Mol. Spectrosc. **195**, 229 (1999).
[50]J. Wu, J. Ma, Y. Zhang, Y. Li, L. Wang, Y. Zhao, G. Chen, L. Xiao, and S. Jia, Phys. Chem. Chem. Phys. **13**, 18921 (2011).
[51]H. Wang and W. C. Stwalley, J. Chem. Phys. **108**, 5767 (1998).
[52]W. Liu, J. Wu, J. Ma, P. Li, V. B. Sovkov, L. Xiao, and S. Jia, Phys. Rev. A **94**, 032518 (2016).
[53]W. C. Stwalley, Eur. Phys. J. D **31**, 221 (2004).
[54]J. Ma, L. Wang, Y. Zhao, L. Xiao, and S. Jia, J. Mol. Spectrosc. **255**, 106 (2009).
[55]Y. Zhang, J. Ma, J. Wu, L. Wang, L. Xiao, and S. Jia, Phys. Rev. A **87**, 030503(R) (2013).
[56]J. Ma, J. Wu, G. Chen, Q. Fan, H. Feng, X. Dai, W. Sun, L. Xiao, and S. Jia, J. Phys. Chem. Lett. **4**, 3612 (2013).
[57]P. J. Zabawa, "Production of ultracold, absolute vibrational ground state NaCs molecules," Ph.D. thesis, Department of Physics and Astronomy, University of Rochester, Rochester, New York, 2012.
[58]W. Liu, X. Wang, J. Wu, X. Su, S. Wang, V. B. Sovkov, J. Ma, L. Xiao, and S. Jia, Phys. Rev. A **96**, 022504 (2017).